Project 2328 | October 2024

SJSU SAN JOSÉ STATE UNIVERSITY

MTI MINETA TRANSPORTATION INSTITUTE

Effects of Low-Cycle Fatigue Fracture of Longitudinal Reinforcing Steel Bars on the Seismic Performance of Reinforced Concrete Bridge Piers

Yu-Fu Ko, PhD, PE
Jessica Gonzalez, EIT

CSUTC California State University Transportation Consortium

CALIFORNIA STATE UNIVERSITY LONG BEACH

MINETA TRANSPORTATION INSTITUTE

Founded in 1991, the Mineta Transportation Institute (MTI), an organized research and training unit in partnership with the Lucas College and Graduate School of Business at San José State University (SJSU), increases mobility for all by improving the safety, efficiency, accessibility, and convenience of our nation's transportation system. Through research, education, workforce development, and technology transfer, we help create a connected world. MTI leads the Mineta Consortium for Transportation Mobility (MCTM) and the Mineta Consortium for Equitable, Efficient, and Sustainable Transportation (MCEEST) funded by the U.S. Department of Transportation, the California State University Transportation Consortium (CSUTC) funded by the State of California through Senate Bill 1 and the Climate Change and Extreme Events Training and Research (CCEETR) Program funded by the Federal Railroad Administration. MTI focuses on three primary responsibilities:

Research

MTI conducts multi-disciplinary research focused on surface transportation that contributes to effective decision making. Research areas include: active transportation; planning and policy; security and counterterrorism; sustainable transportation and land use; transit and passenger rail; transportation engineering; transportation finance; transportation technology; and workforce and labor. MTI research publications undergo expert peer review to ensure the quality of the research.

Education and Workforce Development

To ensure the efficient movement of people and products, we must prepare a new cohort of transportation professionals who are ready to lead a more diverse, inclusive, and equitable transportation industry. To help achieve this, MTI sponsors a suite of workforce development and education opportunities. The Institute supports educational programs offered by the Lucas Graduate School of Business: a Master of Science in Transportation Management, plus graduate certificates that include High-Speed and Intercity Rail Management and Transportation Security Management. These flexible programs offer live online classes so that working transportation professionals can pursue an advanced degree regardless of their location.

Information and Technology Transfer

MTI utilizes a diverse array of dissemination methods and media to ensure research results reach those responsible for managing change. These methods include publication, seminars, workshops, websites, social media, webinars, and other technology transfer mechanisms. Additionally, MTI promotes the availability of completed research to professional organizations and works to integrate the research findings into the graduate education program. MTI's extensive collection of transportation-related publications is integrated into San José State University's world-class Martin Luther King, Jr. Library.

Report 24-30

Effects of Low-Cycle Fatigue Fracture of Longitudinal Reinforcing Steel Bars on the Seismic Performance of Reinforced Concrete Bridge Piers

Yu-Fu Ko, PhD, PE

Jessica Gonzalez, EIT

October 2024

A publication of the
Mineta Transportation Institute
Created by Congress in 1991

College of Business
San José State University
San José, CA 95192-0219

TECHNICAL REPORT DOCUMENTATION PAGE

1. Report No. 24-30	**2. Government Accession No.**	**3. Recipient's Catalog No.**	
4. Title and Subtitle Effects of Low-Cycle Fatigue Fracture of Longitudinal Reinforcing Steel Bars on the Seismic Performance of Reinforced Concrete Bridge Piers		**5. Report Date** October 2024	
		6. Performing Organization Code	
7. Authors Yu-Fu Ko, PhD, PE Jessica Gonzalez, EIT		**8. Performing Organization Report** CA-MTI-2328	
9. Performing Organization Name and Address Mineta Transportation Institute College of Business San José State University San José, CA 95192-0219		**10. Work Unit No.**	
		11. Contract or Grant No. ZSB12017-SJAUX	
12. Sponsoring Agency Name and Address State of California SB1 2017/2018 Trustees of the California State University Sponsored Programs Administration 401 Golden Shore, 5th Floor Long Beach, CA 90802		**13. Type of Report and Period Covered**	
		14. Sponsoring Agency Code	
15. Supplemental Notes 10.31979/mti.2024.2328			

16. Abstract

Earthquakes, which can cause tremendous local stress and strain on infrastructure, can cause reinforced concrete (RC) bridges to collapse due to the concrete cracking and fracture of the steel reinforcement rebars. The fracture of longitudinal reinforcing steel due to low-cycle fatigue is one of the main causes of failure in RC structures under earthquake loading. The purpose of this research is to include the effects of low-cycle fatigue fracture of longitudinal reinforcing steel bars on the seismic performance of reinforced concrete bridge piers. To obtain a greater understanding of low-cycle fatigue failure of steel reinforcement of RC bridge piers subjected to seismic loadings, its properties were studied by considering the slenderness ratio to observe its effects on the behaviors of the steel material. The slenderness ratio are functions of unsupported length, diameter of the circular cross section of the longitudinal reinforcing bars, and the spacing of transverse reinforcing bars. The seismic performance of RC single-column pier-supported bridges with flexural failure under near-fault ground motion were assessed with the use of damage indices. The damage indices can numerically assess the damaged state of RC bridge piers and show the gradual accumulation of damage. Four numerical models are developed with fiber-based nonlinear beam-column elements to simulate the damage accumulation on RC bridge piers under seismic loadings, considering variables such as low-cycle fatigue, tensile strain damage, global buckling of longitudinal steel bars, the cracking and spalling of cover concrete, and the bond-slip between concrete and longitudinal steel bars. Bond-slip is related to the interaction between the longitudinal steel rebars and the concrete for load bearing and coordination deformation. The four numerical models were developed with different considerations of low-cycle fatigue and bond-slip: Model 1 (without bond-slip and without fatigue), Model 2 (without bond-slip and with fatigue), Model 3 (with bond-slip and without fatigue), and Model 4 (with bond-slip and with fatigue). The models underwent nonlinear time-history analyses. The results were compared with experimental testing results. All four numerical models are optimal to assess the seismic performance of RC single-column pier-supported bridges. The proposed damage indices can reasonably reflect the damage states in accordance with the experimental results. The proposed models can reasonably predict the damage states and seismic behavior of RC bridge columns and could be available to the structural engineering community for non-linear analysis and performance assessment of RC bridge structures.

17. Key Words Fatigue (Mechanics), Earthquake engineering, Finite element method, Reinforced concrete bridges, Earthquake resistant structures.	**18. Distribution Statement** No restrictions. This document is available to the public through The National Technical Information Service, Springfield, VA 22161.		
19. Security Classif. (of this report) **Unclassified**	**20. Security Classif. (of this page)** **Unclassified**	**21. No. of Pages** 45	**22. Price**

Form DOT F 1700.7 (8-72)

DOI: 10.31979/mti.2024.2328

Mineta Transportation Institute
College of Business
San José State University
San José, CA 95192-0219

Tel: (408) 924-7560
Fax: (408) 924-7565
Email: mineta-institute@sjsu.edu

transweb.sjsu.edu/research/2328

Acknowledgments

This research work was financially supported by the Mineta Transportation Institute (MTI) for Transport Year 6, 2023. The research team would like to sincerely thank MTI for the support received to accomplish this study.

Contents

List of Figures

List of Tables

Executive Summary

Seismic events often cause disruptions to reinforced concrete (RC) bridge structures, resulting in significant economic and other losses. When subjected to tremendous local stress and strain, concrete tends to crack, and steel reinforcement rebars fracture. For these reasons, earthquakes can cause extensive damage to the structural integrity of RC bridges, making assessment of their seismic damage crucial.

The steel reinforcement bars within RC bridge piers experience strain reversals under seismic loadings. Thus, bar global buckling, tensile strain damage, and low-cycle fatigue fractures are major causes of failure. These damage parameters are considered in this study. To assess the seismic performance of RC single-column pier-supported bridges, four numerical models were developed. Finite element models were developed in the Open System for Earthquake Engineering Simulation (OpenSees) program for nonlinear analysis.

These models use fiber-based, nonlinear beam-column elements and were developed with different considerations of low-cycle fatigue and bond-slip: Model 1 (without bond-slip and without fatigue), Model 2 (without bond-slip and with fatigue), Model 3 (with bond-slip and without fatigue), and Model 4 (with bond-slip and with fatigue). The models underwent nonlinear time-history analyses. The models consider different damage parameters such as low-cycle fatigue, tensile strain damage, global buckling of longitudinal steel bars, cracking and spalling of cover concrete, and bond-slip between concrete and longitudinal steel bars.

The RC cross section is divided into cover concrete, core concrete, and reinforcing steel. The cross sections are made up of fiber cells which are assigned uniaxial constitutive models that have nonlinear material properties representing stress-strain hysteresis behavior. The fibers in OpenSees are titled “concrete02” to represent the concrete and the Hysteretic material model to represent the reinforcing steel which can record the stress-strain hysteresis behaviors. Model 2 and Model 4 had an additional damage fatigue parameter attached to the Hysteretic material to observe its effect. It should be noted that shear failure is assumed not to be governed. The bridge column in this study is assumed to be flexural failure. The bridge pier was modeled with finite element nodes and elements in between the nodes. Model 3 and Model 4 were given a zero-length section element at the base of the RC bridge column to observe the bond-slip effect. The bridge pier of all four numerical models was represented with nonlinear fiber-based and displacement-based beam-column elements with distributed plasticity which allows for nonlinearities to occur anywhere along the member. This allows the user to precisely record its seismic response.

The four proposed models underwent nonlinear time-history analyses, where their stress and strains were recorded for each fiber. This allowed for continuous monitoring of cover concrete spalling and reinforcing steel damage states. The simulation results of the four proposed models are compared with experimental test results. Based on the simulation results, the various damage indices of the RC bridge column are calculated, falling in a range between 0.0 and 1.0, which

corresponds to the structural damage condition based on National Cooperative Highway Research Program (NCHRP) Synthesis.

The proposed numerical models increase the accuracy of the nonlinear, flexural failure behaviors of RC single-column pier-supported bridges under seismic ground motions. The damage indices are in accordance with the experimental results, making the models useful for those performing non-linear analysis and performance assessment of RC bridge structures.

1. Introduction

During the 1971 San Fernando earthquake in California, more than 60 bridges on the Golden State Freeway in California were damaged. The San Fernando earthquake cost the state approximately $100 million in bridge repairs. The Loma Prieta earthquake in 1989 damaged more than 80 bridges in California and caused more than 40 deaths in bridge-related collapses alone. The cost of bridge damage by Loma Prieta earthquake was about $300 million. Earthquake-damaged bridges have major impacts on transportation systems. Therefore, it is imperative to propose numerical models that can accurately predict the seismic behavior of reinforced concrete (RC) bridges as well as assess their damage states.

Many seismic damage indices have been developed in literature to assess the structural damage induced by earthquakes [1–6]. Park and Ang's damage model is a function of maximum deformation and the absorbed hysteretic energy [2,3]. Babazadeh et al. use 3D continuum-based finite element simulations to predict intermediate damage limit states of RC bridge columns but do not consider bond-slip effects, as a perfect bond between the reinforcement and concrete is assumed [7].

In addition, researchers have shown that low-cycle fatigue-induced damage is a prominent mode of rebar failure under seismic conditions. Heo and Kunnath developed a fiber-based damage model which considers low-cycle fatigue in their reinforcing steel fibers, but other parameters such as damage caused by displacement are not included [4]. Furthermore, Kashani et al. [8] conducted fiber-based nonlinear analysis to predict the nonlinear responses of RC bridge piers with fewer computational efforts, despite considering bar global buckling and low-cyclic fatigue of longitudinal reinforcing steel. But they did not use any damage indices or clear damage assessment protocol. Tripathi M. et al. studied the combined effect of low-cycle fatigue and buckling in RC columns. The global buckling of reinforcing bars has detrimental effects on their fatigue life [9]. Su et al. developed fiber-based, nonlinear, finite element models of RC bridge columns to assess bridge column damages [6]. Five damage levels are used to measure the damage states to classify a bridge column's performance levels as recommended by Stone and Taylor [10,11], Goodnight and Nau [12], Mckenna et al. [13], Sharifi et al. [14], and Yue et al. [15].

Ding et al. [16] conducted experimental and numerical investigations on RC bridge piers, considering global buckling and low-cycle fatigue. The experimental study consisted of seven 1/5 scaled rectangular RC bridge piers which were tested under constant axial load and horizontal quasi-static cyclic loading. Their results found that increasing the slenderness ratio intensified the pinching effects of reinforcing steel under cyclic loading. Global buckling and low-cycle fatigue properties of longitudinal bars are the main factors that cause damage failure of RC piers and, thus, have a great impact on the ductility of RC piers. Kashani et al. [17] studied the effect of inelastic buckling on low-cycle fatigue life of steel reinforcing bars by conducting experimental testing on ninety reinforcing bars of sizes 12 mm and 16 mm with different buckling lengths and strain amplitudes. The inelastic buckling has a great influence on the stress–strain relationship of

reinforcing bars. Additionally, when they increased the buckling length of the bars, the low-cycle fatigue life decreased, which indicates that their energy dissipation capacity under cyclic loading also decreased. Moreover, the 16 mm diameter bars reached a fractured state earlier than the 12 mm diameter bars, suggesting that the bar diameter also affects the low-cycle fatigue life of reinforcing bars. Su et al. [18] studied the seismic behavior of RC bridge piers and the influence of low-cycle fatigue damage of reinforcing bars under spectrally equivalent short- and long-duration ground motions. They developed finite element models that considered global buckling and low-cycle fatigue of longitudinal bars that underwent nonlinear dynamic analysis. They concluded that the low-cycle fatigue damage of reinforcing bars is a significant cause of failure in RC bridge columns and should be considered in the seismic design.

Near-fault earthquakes are a concern as they produce pulse-like velocity waveforms that are destructive to structures. There have been experimental testing and numerical simulations of RC bridge columns under near-fault earthquakes [19–26]. Chang et al. [19] conducted pseudo-dynamic testing of three RC bridge piers under cyclic loading to estimate their shear strength, flexural strength, and ductility. Pang et al. [25] evaluated the seismic performance of bridge piers, considering both flexural and brittle failure mechanisms at different damage states under both far-field and near-fault ground motions. The study developed a 3-D finite element model for an RC bridge pier to perform nonlinear time history analysis. It selected 30 near-fault and 30 far-field ground motions and compared the results. The results concluded that the near-fault records increased the seismic demands when compared to far-field earthquakes.

Phan et al. [27] studied the characteristics of near-fault earthquakes on RC bridge columns by designing two large-scale columns and testing them under a near-fault ground motion on a shake table. The results found that near-fault earthquake records tend to contain an asymmetrical, high-amplitude velocity pulse that causes whiplike behavior in columns and causes large displacements in one direction. As a result, significant residual displacement is developed. Todorov et al. [28] developed a fiber-based, nonlinear, finite element model of a bridge pier to evaluate the damage potential of different near- and far-field earthquakes. The study found that bridge piers under pulse-like motions tend to collapse much earlier before reaching their collapse limit state.

However, numerical models proposed by prior researchers have not been developed to deal explicitly with various combined damage mechanisms observed through the experimental tests for RC bridge columns, especially the combination of low-cycle fatigue and global buckling of longitudinal reinforcing bars with bond-slip effect. The proposed research study will fill the gaps by considering various damage parameters to assess the seismic performance of RC bridges as well as the near-fault ground motion effects.

Earthquakes can cause RC bridges to collapse due to the concrete cracking and fracture of the steel reinforcement rebars when they are subjected to tremendous local stress and strain. The fracture of longitudinal reinforcing steel due to low-cycle fatigue is one of the main causes of failure in RC structures under earthquake loading. Therefore, the purpose of this research is to investigate the

effects of low-cycle fatigue fracture of longitudinal reinforcing steel bars on the seismic performance of RC bridge piers as well as to assess the seismic damage of bridge columns.

Plastic deformation in each cycle and low-cycle phenomenon (materials have finite endurance for this type of load) are the characteristics of low-cycle fatigue. The term "cycle" refers to repeated applications of stress that lead to eventual fatigue and failure. "Low-cycle" pertains to a long period between applications. The low-cycle fatigue assessment results will allow us to better understand the behavior of RC bridges under seismic motions.

The aim of this research is to evaluate the seismic performance of RC single-column pier-supported bridges and the influence from low-cycle fatigue of longitudinal reinforcing bars. To obtain a greater understanding of the low-cycle fatigue failure of steel reinforcement of RC bridge piers subjected to seismic loadings, low-cycle fatigue failure was also studied by considering the slenderness ratio to observe its effects on the behaviors of the steel material. The slenderness ratio are functions of unsupported length, the diameter of the circular cross section of the longitudinal reinforcing bars, and the spacing of transverse reinforcing bars. The seismic performance of RC single-column pier-supported bridges with flexural failure under near-fault ground motion was assessed with the use of damage indices. The damage indices numerically assess the damaged state of RC bridge piers and show the gradual accumulation of damage. Four numerical models were developed with fiber-based, nonlinear, beam-column elements to simulate the damage accumulation on RC bridge piers under seismic loadings, considering the low-cycle fatigue, tensile strain damage, global buckling of longitudinal steel bars, cracking and spalling of cover concrete, and the bond-slip between concrete and longitudinal steel bars. The four numerical models were developed with different considerations of low-cycle fatigue and bond-slip: Models 1 (without bond-slip and without fatigue), Model 2 (without bond-slip and with fatigue), Model 3 (with bond-slip and without fatigue), and Model 4 (with bond-slip and with fatigue).

The proposed numerical models developed are based on a single RC bridge column that is fixed at the base and free at the top, as shown in Figure 1. The RC bridge column is assessed with the use of damage indices. The proposed models consider the bond-slip effect between the concrete and the longitudinal reinforcing bars [29–31], buckling of the longitudinal reinforcing bars [32–34] concrete cracking and spalling [34–35], and low-cycle fatigue of longitudinal reinforcing bars [16–18]. The simulation results of the four proposed models were compared with experimental test results by Chang et al. [19] to predict the seismic behavior of RC bridges and assess the damage states of RC bridges. This experimental data was selected as it includes comprehensive experimental investigation of the seismic response of the scaled modern RC bridge column.

Figure 1. RC Single Column Bridge Pier

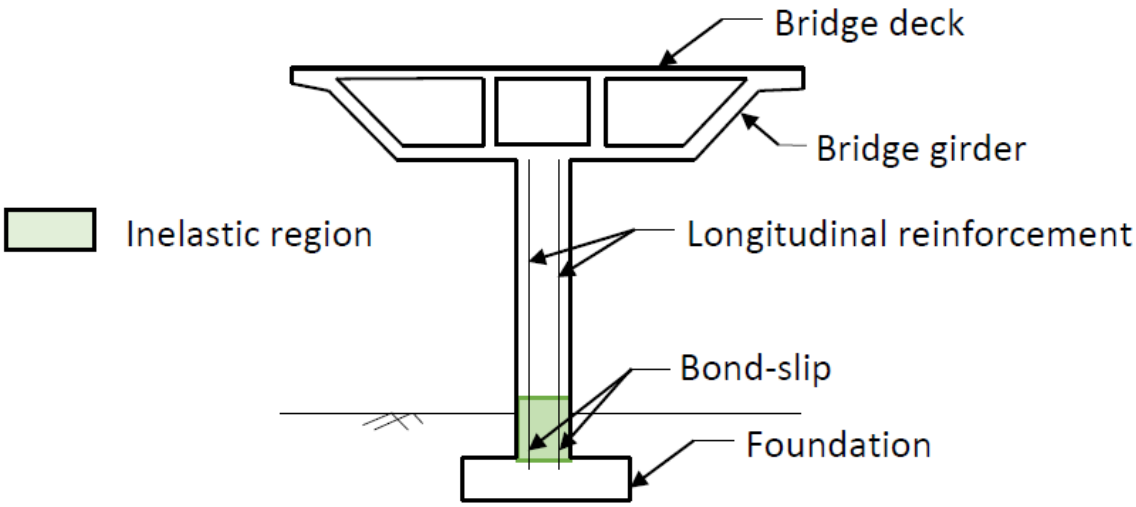

2. Specimen and Testing Method from Experimental Study

The RC bridge column selected was Specimen B from Chang et al.'s pseudo-dynamic tests and represents an as-built RC bridge column. Specimen B is a scaled RC bridge column at a 2/5 reduction and was designed using 1995 Taiwan Bridge Design Code, which is based on the 1992 AASHTO specifications.

The height of the bridge columns was 3.25 m, and the cross section was 0.75 m by 0.60 m, which includes a 25 mm concrete cover. The longitudinal reinforcement consisted of 32 No. 6 bars placed evenly along the column's height, with a reinforcement ratio of 1.95%. The longitudinal reinforcement's design's yield strength was f_y = 420 MPa (with an exact yield strength of 500 MPa), and its concrete compressive strength was f'_c = 21 MPa at 28 days (with an exact strength of f_y =23 MPa). The transverse reinforcement consisted of No. 3 stirrups spaced at 100 mm, with a design yield strength of f_y = 280 MPa (and an exact strength of f_y = 350 MPa) and a reinforcement ratio of 1.04%. In addition, the transverse reinforcement included five confining crossties. The hoops were anchored at their two ends at 90°. The crossties were anchored at their two ends at 135°. The bridge column was subjected to an axial compressive load of 680 kN.

Specimen B was subjected to the Taiwan 1999 Chi-Chi earthquake's horizontal ground acceleration whose ground motion was acquired from station TCU075, and the peak ground acceleration (PGA) was scaled up to 0.8 g. The maximum force, maximum lateral displacement, and ductility capacity were recorded. Specimen B underwent pseudo-dynamic loading to attain the precise seismic demands and responses of RC bridge columns under near-fault ground motion. The pseudo-dynamic results of Specimen B were calibrated with the simulation results of the proposed four numerical models.

3. Low-Cycle Fatigue Effects on Steel Reinforcing Materials

In OpenSees [13], the fatigue effect could be considered by different approaches. One approach is to adopt the ReinforcingSteel material with the consideration of fatigue, which is denoted at the end of the command as -CMFatigue. Another approach is to wrap Fatigue material to Hysteretic material for steel material. "Wrap" is defined as integrating the new material with the parent material. The Fatigue material "wraps" around the Hysteretic material and does not influence the stress-strain (or force-deformation) relationship of the parent material. A modified rainflow cycle counter was implemented to track strain amplitudes. This cycle counter was used in concert with a linear strain accumulation model (i.e., Miner's Rule), based on the Coffin-Manson log-log relationships, describing low-cycle fatigue failure.

The fatigue modeling in OpenSees uses the Coffin-Manson fatigue life relationship based on strain amplitude and number of cycles:

$$\varepsilon_p = C_f (2N_f)^{-\alpha} \quad (1)$$

where C_f is the Coffin-Manson constant, α is the cyclic strength reduction constant, ε_p is the plastic strain amplitude, and $2N_f$ represents the number of half-cycles to failure corresponding to the plastic strain amplitude. Miner's linear damage rule was then applied to determine the cumulative damage in reinforcing steel.

To demonstrate the fatigue effects on steel reinforcing materials, the ReinforcingSteel material with -CMFatigue in OpenSees was adopted. The fatigue command requires parameters C_f (ductility constant used to adjust the number of cycles to failure), α (Coffin-Mason constant), and C_d (strength reduction constant). Combinations of these parameters are shown in Figure 2 to compare the strength degradation of reinforcing steel bars due to C_f, α, and C_d values. Figure 2a keeps α and C_d as constants with a varied C_f value to observe the effect of C_f. Figure 2b compares the fatigue property change with a varied C_d value while keeping α and C_f as constants. Figure 2c demonstrates the effect of α values on the fatigue property with C_f and C_d as constants. The results demonstrate that each fatigue parameter influences cyclic behavior of steel rebar.

Figure 2. Comparison of Fatigue Parameters: (a) Varied C_f; (b) Varied C_d; (c) Varied α

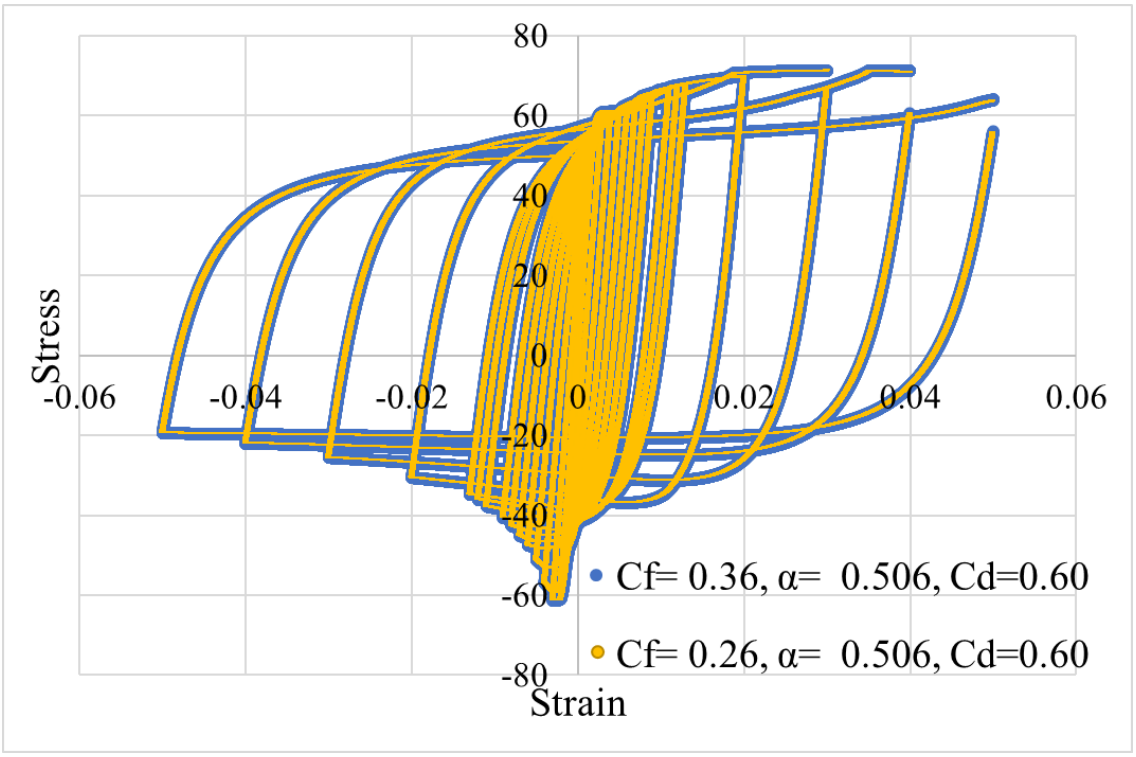

(a)

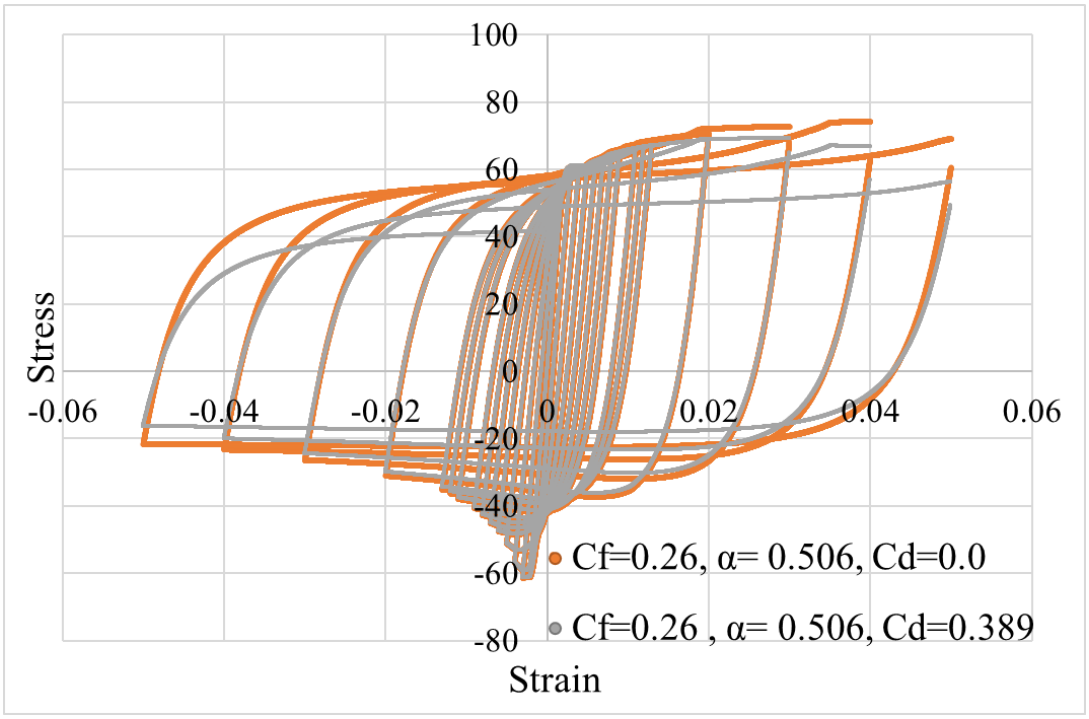

(b)

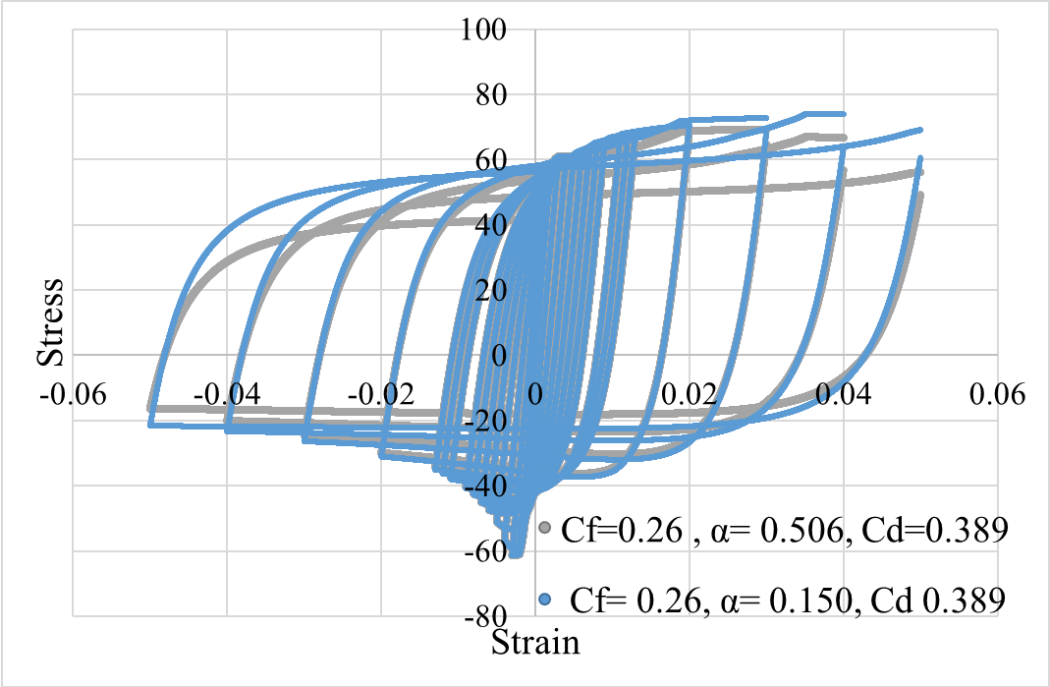

(c)

Furthermore, in this research, the proposed fiber-based damage models also considered the effect of global buckling with various slenderness ratios of longitudinal reinforcing bars (L/D) incorporated in the fatigue modeling by wrapping Fatigue material to Hysteretic material for steel material.

The low-cycle fatigue of reinforcing bars including the effects of global buckling can be evaluated by Equation (2), where the fatigue life coefficients can be obtained using Equation (3) and Equation (4):

$$\varepsilon_p = E_0(2N_f)^m \quad (2)$$

$$\lambda = L/D\sqrt{fy/100} \quad (3)$$

$$E_0 = (-\lambda/350) + 0.20;\ m = -(\lambda/1200 + 0.441) \quad (4)$$

In Equation (2), the ε_p, E_0, m, and $2N_f$ represent the plastic strain amplitude, fatigue ductility coefficient, fatigue ductility exponent, and number of half cycles to failure, respectively. The effect of global buckling is included by expressing the fatigue coefficients (E_0, m) as a function of global buckling parameter (λ), defined in Equation (3) [33]. The global buckling parameter is an expression between the slenderness ratio and yielding stress.

4. Material Damage Models and Finite Element Models with Low-Cycle Fatigue

4.1 Definitions of Damage Indices and Performance Assessment

The damage indices of RC bridges, as shown in Figure 3, are numerically determined in a range of 0.0 to 1.0. This range corresponds to the structure damage, as seen in Table 1 [11] and is derived from the NCHRP Synthesis [36]. The damage value for each damage level is adopted for the numerical models proposed in this study. The damage level of RC bridges can be assessed and measured as shown in Table 2 [36]. There are five distinct levels of qualitative and quantitative performance characterizations used to measure the RC bridge performance. The qualitative descriptions for RC bridge columns include crack widths and lengths. The tensile strain of longitudinal bars is the reason for concrete crack widths. The onset of yielding in longitudinal steel bars is the first major sign of damage in RC bridge columns. This yielding is the marker of Level II and corresponds to damage values between 0.1 and 0.2. The next sign of damage in RC bridge columns is the onset of cover concrete spalling, which is equivalent to the crack length extending to one-tenth of the section depth in Level III. In Level IV, significant spalling corresponds to concrete crack widths larger than 2 mm that extend over half of the cross section. In Level V, the last sign of damage is the buckling of main reinforcement and the crushing of the core concrete.

Table 1. Assessment of Bridge Performance [11]

Level	Performance level	Qualitative performance characterization	Quantitative performance characterization
I	Cracking	Onset of hairline cracks	Cracks hardly visible
II	Yielding	Theoretical first yielding of longitudinal reinforcement	Crack widths <1 mm
III	Initiation of local mechanism	Initiation of inelastic deformation, onset of concrete spalling, development of diagonal cracks	Crack widths of 1–2 mm, length of spalled region >1/10 of the cross-section's depth
IV	Full development of local mechanism	Wide and extended cracks, significant spalling over local mechanism region	Crack widths >2 mm, diagonal cracks extend over 2/3 of the cross-section's depth Length of spalled region >1/2 of the cross-section's depth
V	Strength degradation	Buckling of main reinforcement, Rupture of transverse reinforcement, Crushing of core concrete	Crack widths >2 mm in core concrete

Table 2. Damage Index Levels Classifications [36]

Level	Damage Classification	Damage Value	Description	Performance Condition
I	None	D < 0.1	Onset of hairline cracks	Fully operational
II	Minor	0.1 ≤ D< 0.2	Crack widening, first yielding of reinforcement	Operational
III	Moderate	0.2 ≤ D< 0.4	Onset of cover concrete spalling	Limited damage
IV	Major	0.4 ≤ D< 0.6	Significant spalling	Life safety
V	Local Failure/Collapse	0.6 ≤ D< 1.0	Buckling of reinforcement, crushing of core concrete	Collapse

Figure 3. Definitions of Damage Indices

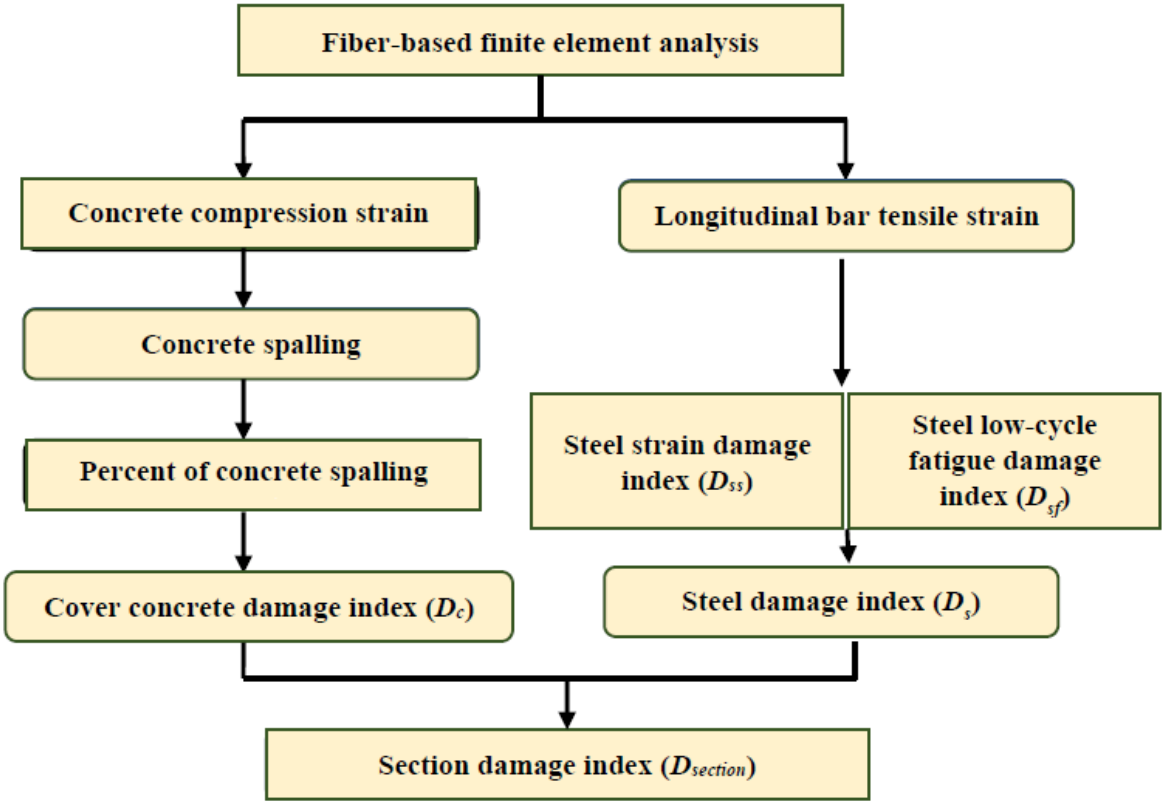

Figure 4. Definition of Cover Concrete Spalling [19]

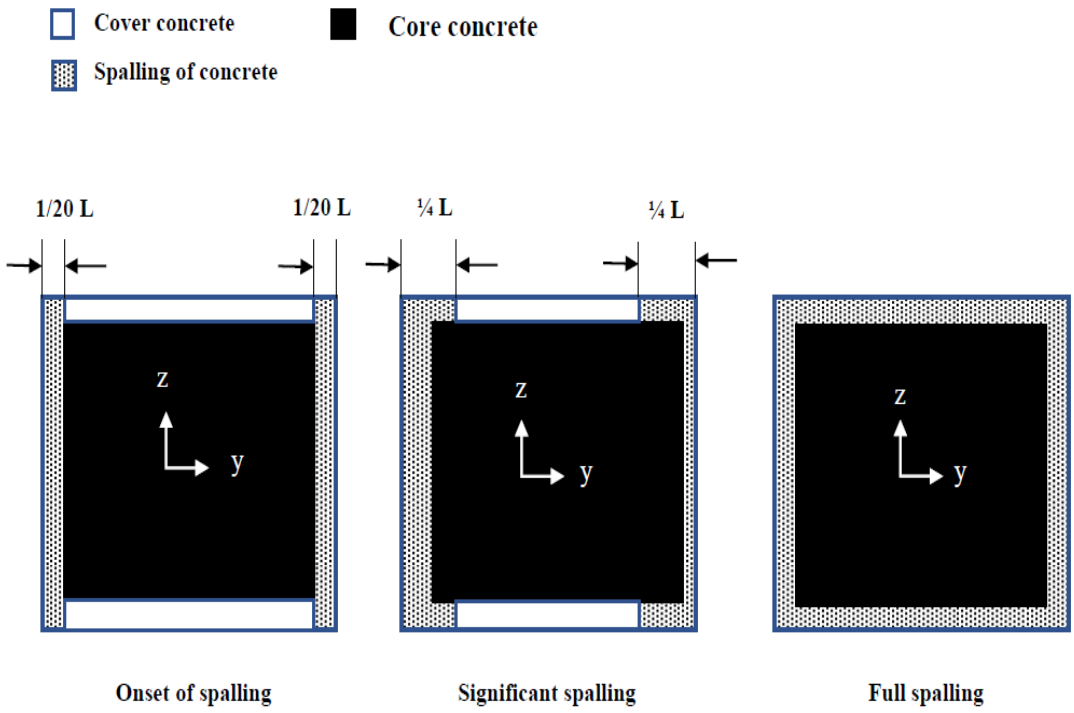

Figure 5. Concrete and Steel Fiber Numbering in the Cross Section

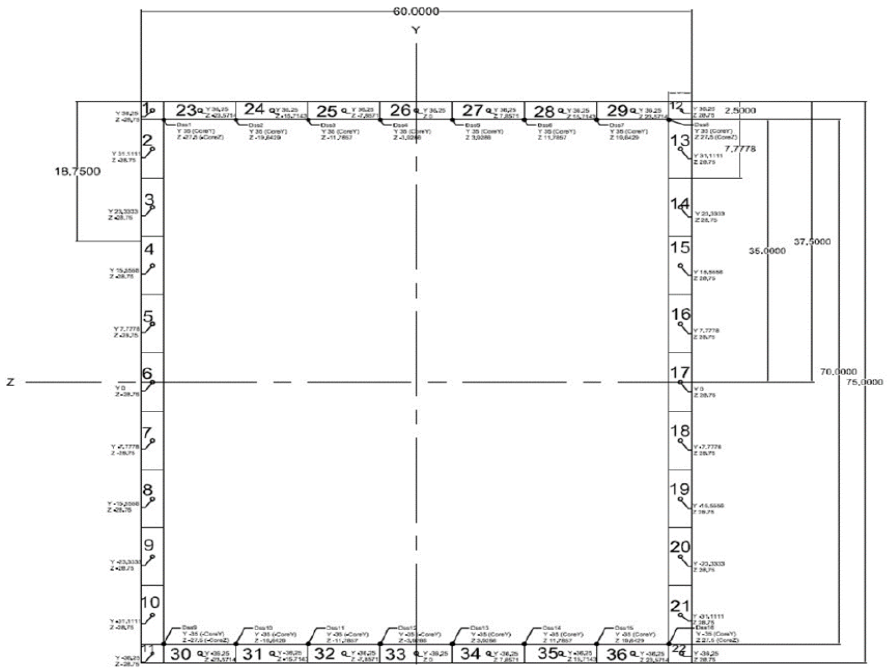

4.1.1 Fiber-Based Material Damage Models

To perform nonlinear time-history analyses and assess the damage states of RC bridge columns, the proposed fiber-based damage models were coded in the OpenSees program [13]. The RC bridge column and its cross sections were divided into fiber cells and were allocated uniaxial constitutive models with nonlinear material properties, which can depict the stress-strain hysteresis models for concrete and longitudinal rebar. The RC cross section was divided into cover concrete, core concrete, and reinforcing steel sections. For cover concrete and core concrete in the proposed numerical models, the Concrete02 material [37] in OpenSees was used. To simulate the longitudinal reinforcing bars in the bridge columns, the uniaxial bilinear material Hysteretic in OpenSees was adopted. The steel material took into account the mechanical effects of low-cycle fatigue, strain softening, compression global buckling, and tensile fracture of the reinforcement bars. Fatigue material was wrapped to Hysteretic material for steel material. The fatigue material model in the OpenSees program is a fatigue life model based on the Coffin-Manson log-log relationships, which utilizes the modified rainflow cycle counting algorithm to track the accumulated damage in the steel material.

4.1.2 Cover Concrete Damage Index

The cover concrete damage of RC bridge columns is associated with the extent of cover concrete spalling because of the deterioration in its RC cross sections. The section damage of cover concrete is determined as:

$$D_c = \begin{cases} p/p_1 * D_{s1}, p < p_1 \\ D_{sc1} + (p - p_1)/(p_2 - p_1) * (D_{sc2} - D_{sc1}), p_1 < p \leq p_2 \\ D_{sc2} + (p - p_2)/(p_3 - p_2) * (D_{sc3} - D_{sc2}), p_2 < p \leq p_3 \end{cases} \quad (5)$$

The variable p represents the percentage of cover concrete spalling. The damage indices D_{sc1} to D_{sc3} are 0.2, 0.4, and 0.6, respectively. A compression strain of -0.005 identifies the onset of cover concrete spalling. The cover concrete damage was evaluated in every time step of ground motion recorded to be in either onset spalling, significant spalling, or full spalling, as shown in Figure 4. The percentage, p_1, was computed as the number of fibers that reached or surpassed the strain threshold of -0.005 during the onset of spalling over the total number of fibers. The percentages of the RC rectangular section were determined to be p_1 = 50%, p_2 = 72%, and p_3 = 100%.

4.1.3 Steel Strain Damage Index

The strain-based damage of longitudinal reinforcing steel bars was computed as:

$$D_{ss} = \begin{cases} \frac{\varepsilon_b}{\varepsilon_y} * D_{s1}, \varepsilon_s < \varepsilon_y \\ D_{s1} + (\varepsilon_s - \varepsilon_y)/(\varepsilon_{c1} - \varepsilon_y) * (D_{s2} - D_{s1}), \varepsilon_y \leq \varepsilon_s < \varepsilon_{c1} \\ D_{s2} + (\varepsilon_s - \varepsilon_{c1})/(\varepsilon_{c2} - \varepsilon_{c1}) * (D_{s3} - D_{s2}), \varepsilon_{c1} \leq \varepsilon_s < \varepsilon_{c2} \\ D_{s3} + (\varepsilon_s - \varepsilon_{c2})/(\varepsilon_{bb} - \varepsilon_{c2}) * (D_{s4} - D_{s3}), \varepsilon_{c1} \leq \varepsilon_s < \varepsilon_{bb} \\ D_{s4} + (\varepsilon_s - \varepsilon_{c3})/(\varepsilon_u - \varepsilon_{bb}) * (D_{s5} - D_{s4}), \varepsilon_{bb} \leq \varepsilon_s < \varepsilon_u \\ D_{s5}, \varepsilon_s \geq \varepsilon_u \end{cases} \quad (6)$$

The ultimate strain of the longitudinal steel, ε_u, was fixed to 0.10 for the proposed numerical models. Goodnight et al. [12] determined that the steel strain values, ε_{c1} = 0.01 and ε_{c2} = 0.02 correspond to longitudinal bars with crack widths of 1 mm and 2 mm. The damage classifications, D_{s1} to D_{s5}, were set as 0.1, 0.2, 0.4, 0.6, and 1.0, respectively. In addition, the buckling strain was determined as:

$$\varepsilon_{bb} = 0.03 + 700 p_{sh} \frac{f_{yh}}{E_s} - 0.1 \frac{P}{f'_c A_g} \quad (7)$$

4.1.4 Steel Low-Cycle Fatigue Damage Index

The reinforcing steel bars in bridge piers are prone to fracture due to low-cycle fatigue for flexural members in seismic areas [38]. In OpenSees, the fatigue effect is included by wrapping Fatigue material to the Hysteretic material. The fatigue modeling uses the Coffin-Manson fatigue life relationship based on strain amplitude and the number of cycles:

$$\varepsilon p = Cf\,(2Nf)^{-\alpha} \quad (8)$$

Cf is the Coffin-Manson constant, α is the cyclic strength reduction constant, εp is the plastic strain amplitude, and 2Nf represents the number of half-cycles to failure corresponding to the plastic strain amplitude. Miner's linear damage rule was then applied to determine the cumulative damage in reinforcing steel:

$$D_i = 1/2Nf = (\varepsilon pi / Cf)^{1/\alpha} \quad (9)$$

$$D_{sf} = \Sigma\, D_i \quad (10)$$

4.1.5 Section Damage Index

The steel damage index D_s is the maximum value between the steel low-cycle fatigue damage index D_{sf} and the steel strain damage index D_{ss}, as indicated in Equation (11). The section damage index of the RC bridge column was selected as the greater value between the cover concrete damage index D_c and the steel damage index D_s, as expressed in Equation (12) and Figure 3.

$$D_s = max\{ D_{ss}, D_{sf}\} \quad (11)$$

$$D_{section} = max\{ D_s, D_c\} \quad (12)$$

4.2 Finite Element Models

The development of the fiber-based, finite element models was formed by using the OpenSees program. The rectangular cross section of the RC bridge column was comprised of the following segments: confined core concrete fibers, unconfined cover concrete fibers, and longitudinal reinforcing steel fibers, as shown in Figure 5. The confined and unconfined concrete segments accounted for the effect of closed steel hoops (transverse reinforcing bars) on the concrete. The unconfined concrete fibers were discretized in 36 locations, and the steel fibers were discretized in 16 locations, as shown in Figure 5.

The bridge column of all models consisted of uniaxial nonlinear fibers labeled as "UniaxialMaterial" to depict the stress-strain hysteresis behaviors of concrete and longitudinal reinforcing steel. The cross section aggregate with elastic shear for concrete was ignored, as it was assumed that flexural failure governed over shear failure. The models were composed of finite element nodes, where extra nodes were added between nodes to refine the element length. Since strong seismic loadings were used to predict the bridge column's yielding and damage, nonlinear fiber-based and displacement-based beam-column elements were used between nodes to represent the bridge columns for the proposed four numerical models. To allow for the growth of nonlinearities anywhere along the member, nonlinear fiber-based and displacement-based beam-column elements with distributed plasticity were adopted. The "Recorders" in OpenSees monitored and recorded the seismic responses of RC bridge columns.

4.2.1 Model 1 (without bond-slip and without fatigue)

Uniaxial concrete material Concrete02 in OpenSees was used to represent the confined and unconfined concrete. The longitudinal reinforcing steel bars in the RC fiber section were modeled by using uniaxial, bilinear material Hysteretic after calibration with ReinforcingSteel.

The following conditions were used for the confined concrete material. The concrete compressive strength at 28 days was f'_{cc} = -24.8 MPa, the concrete strain at maximum strength was ε_{cc} = 0.0061, the initial slope for compressive stress–strain curve was $E_c = 5000\sqrt{f'cc}$ = 24,900.0 MPa, the concrete crushing strength was $f_{cu} = 0.4f'_{cc}$ = 9.9 MPa, the concrete strain at crushing strength was ε_{cu} = -0.014, the ratio between unloading slope at ε_{cu} and initial slope was λ = 0.1, the tensile strength of the concrete was $f_t = 0.59\sqrt{f'c}c$ = 2.94 MPa, and the tension softening stiffness (slope of the linear tension softening branch) was $E_{ts} = E_c/10$ = 2490.0 MPa.

The following conditions were used for the unconfined concrete material. A concrete compressive strength at 28 days of f'_c = -23.0 MPa, the concrete strain at maximum strength was ε_0 = -0.002, an initial slope for the compressive stress-strain curve of $E_c = 4700\sqrt{f'c}$ = 22,540.0 MPa, concrete

crushing strength, f_{cu} = 0.0 MPa, the concrete strain at crushing strength, ε_{cu} = -0.004, the ratio between unloading slope at ε_{cu} and initial slope was λ = 0.1, the tensile strength of the concrete is $f_t = 0.59\sqrt{f'c}$ = 2.83 MPa, the tensile strain of 0.00012 at f_t, and the tension softening stiffness was $E_{ts} = E_c/10$ = 2254.0 MPa.

The following conditions were used for the longitudinal reinforcing rebars of the ReinforcingSteel material. The yield strength in tension was f_y = 420 MPa, the ultimate strength was $f_u = 1.19f_y$, the strain corresponding to initial strain hardening was ε_{sh} = 0.008, the strain at peak stress was ε_{su} = 0.14, the initial elastic tangent modulus was E_s = 200, 000.0 MPa, and the tangent at initial strain-hardening modulus was E_{sh} = 7000.0 MPa.

The buckling simulations of the longitudinal rebars were adopted from Gomes and Appleton [32] and Dhakal and Maekawa [33]. The slenderness ratio was defined as $l_{SR} = 1.5 * L_u/d_b = 1.5 * s/d_b$. The L_u, d_b, and s variables are the unsupported length, the diameter of the circular cross section of the longitudinal reinforcing bars, and the spacing of transverse reinforcing bars, respectively. The buckled stress σ_b is expressed as:

$$\sigma_b = \gamma f_u - \frac{\Omega_b + \gamma}{1+\gamma}(\gamma f_u - \sigma); \ \Omega_b = \beta \frac{\sqrt{32}}{(3\pi \, l_{SR}\sqrt{\varepsilon_s - \varepsilon_y})} \quad (13)$$

where amplification factor β = 1.0, a buckling reduction factor r = 0.0, and a buckling constant γ = 0.5; the variables σ_b is the buckled stress, ε_y is the yield strain, and fu is the ultimate strength of the ReinforcingSteel material in tension.

After the calibration of the Hysteretic material with the ReinforcingSteel material by considering global buckling of longitudinal reinforcing bars, the Hysteretic command was assigned to the steel fibers. The Hysteretic material uses six stress and strain points as inputs along with pinching constants, damage due to ductility and energy, and degradation unloading stiffness based on ductility.

Furthermore, nonlinear fiber-based and displacement-based beam-column elements were used instead of a lumped plastic hinge to consider the spread of plasticity along the element. Six displacement-based beam-column elements were the most fitting choice after performing the element refinement studies and convergence tests. The integration along the element follows the Gauss-Lobatto quadrature rule.

4.2.2 Model 2 (without bond-slip and with fatigue)

Model 2 was set up like Model 1, but with the inclusion of low-cycle fatigue of longitudinal reinforcing bars. After the calibration of the Hysteretic material with the ReinforcingSteel material by considering both global buckling and low-cycle fatigue of longitudinal reinforcing bars, the Hysteretic command was assigned to the steel fibers. The Hysteretic material uses six stress and

strain points as inputs along with pinching constants, damage due to ductility and energy, and degradation unloading stiffness based on ductility.

Furthermore, in this research, Model 2 also considered the effect of global buckling with various slenderness ratios of longitudinal reinforcing bars (L/D) incorporated in the fatigue modeling by wrapping Fatigue material to Hysteretic material for steel material.

The fatigue properties were calculated as described in Section 3. The fatigue properties applied were for L/D = 7, which equate to E_0 = 0.159 and m = -0.453.

The low-cycle fatigue of reinforcing bars including the effects of global buckling were evaluated in Equation (2), where the fatigue life coefficients were obtained using Equations (3) and (4).

4.2.3 Model 3 (with bond-slip and without fatigue)

Model 3 was modified from Model 1 by adding a zero-length section at the base of the bridge column to include the bond-slip effect. The concrete material within the zero-length section was identical to the concrete material used in the fiber-based beam-column elements. The reinforcing steel in the zero-length section applied the Bond_SP01 uniaxial material in OpenSees to mimic the bond-slip effects at the column-to-footing intersection [31]. The monotonic bar stress (σ) versus loaded-end slip (S) response curve in Bond_SP01 was expressed in Equations (14) and (15) as:

$$\sigma = \begin{cases} KS, if\ S \le S_y \\ \tilde{\sigma}\ \mathrm{x}\ (\sigma_u - \sigma_y) + \sigma_y, if\ S > S_y \end{cases}; \tilde{\sigma} = \frac{\frac{\tilde{S}}{\mu - \tilde{S}}}{[(\frac{1}{\mu x b})^{Rc} + (\frac{\tilde{S}}{\mu - \tilde{S}})^{Rc}]^{1/Rc}} \quad (14)$$

where b is the stiffness reduction factor, which expresses the ratio of the initial slope of the curvilinear portion at the onset of yielding to the slope in the elastic region, K. The variable $\tilde{\sigma} = (\sigma - \sigma_y)/(\sigma_u - \sigma_y)$ is the normalized bar stress, $(\tilde{S}) = (S - S_y)/S_y$ is the normalized bar slip, $\mu = (S_u - S_y)/S_y$ is the ductility coefficient, The variable σ_y is the yield strength, and σ_u is the ultimate strength of the bar reinforcement. S_y and S_u are the loaded end-slip corresponding to the bar stress σ_y and σ_u, respectively. S_y is computed as follows:

$$S_y = 0.4\left[\frac{d_b}{4}\frac{Fy}{\sqrt{f'_c}}(2\alpha + 1)\right]^{1/\alpha} + 0.34\ (\mathrm{mm, Mpa}) \quad (15)$$

The coefficient R_c generates the shape of the reloading curve in the hysteretic responses of bar stress versus loaded-end slip, and typically R_c ranges from 0.5–1.0. A lower R_c value generates significant pinching behavior, while a value of 1.0 will render no pinching effect. The following parameters were adopted for Bond_SP01: the local bond-slip relation (α = 0.4), rebar slips at the loaded end at the bar fracture strength ($S_u = 30S_y$), coefficient to reflect the pinching effect (R_c = 0.23), and the stiffness reduction factor (b = 0.05).

4.2.4 Model 4 (with bond-slip and with fatigue)

Model 4 was the combination of Models 2 and 3. Both bond-slip and low-cycle fatigue of longitudinal rebars were considered in Model 4.

A zero-length section was added at the base of the bridge column to include the bond-slip effect. Furthermore, after calibration of the Hysteretic material with the ReinforcingSteel material by considering both global buckling and low-cycle fatigue of longitudinal reinforcing bars, the Hysteretic command was assigned to the steel fibers. The Hysteretic material uses six stress and strain points as inputs along with pinching constants, damage due to ductility and energy, and degradation unloading stiffness based on ductility.

Furthermore, in this research, Model 4 also considered the effect of global buckling with various slenderness ratios of longitudinal reinforcing bars (L/D) incorporated in the fatigue modeling by wrapping Fatigue material to Hysteretic material for steel material.

The low-cycle fatigue of reinforcing bars including the effects of global buckling were evaluated in Equation (2), where the fatigue life coefficients were obtained using Equations (3) and (4). The fatigue properties were calculated as described in Section 3. The fatigue properties employed were L/D = 7, which equates to E0 = 0.159, and m = -0.453.

5. Numerical Investigations on the Seismic Performance of RC Bridge Pier

The proposed four numerical models were subjected to nonlinear time-history analyses due to horizontal ground acceleration with a constant axial compressive load. The proposed four numerical models were developed as a single degree of freedom structure with constant axial compressive load of P = -680 kN. The near-fault Taiwan 1999 Chi-Chi earthquake from station TCU075 was selected for the nonlinear time-history analysis of Specimens B from Chang et al. [19]. The TCU075 earthquake was documented in the following way: Chi-Chi, Taiwan, record sequence #: 1510, event name: RSN1510_CHICHI_TCU075-E, unscaled PGA: 0.233 g, and unscaled time duration: 90 s. The simulation results of the proposed finite element models were calibrated with the experimental test results of Specimen B.

The recorded time history of ground acceleration (g), ground velocity (cm/sec.), and ground displacement (cm) of scaled TCU075 are shown in Figures 6. The peak ground acceleration of TCU075 was scaled up to 0.8 g. Subsequently, the time of duration was compressed due to the similitude law. The scaled-up ground acceleration was implemented with a damping ratio of 5%. Notably, the selected near-fault ground motions revealed that they have pulse-like velocity waveform and a large pulse near the beginning of the velocity time history in Figure 6b. Near-fault ground motions often contain some special characteristics including the high permanent ground displacement and long-period velocity pulses. Therefore, near-fault ground motions have the potential to cause severe damage to RC bridges.

Figure 6. Ground Motion of TCU075 Scaled: (a) Ground Acceleration (g) vs. Time (sec); (b) Ground Velocity (cm/sec) vs. Time (sec); (c) Ground Displacement (cm) vs. Time (sec)

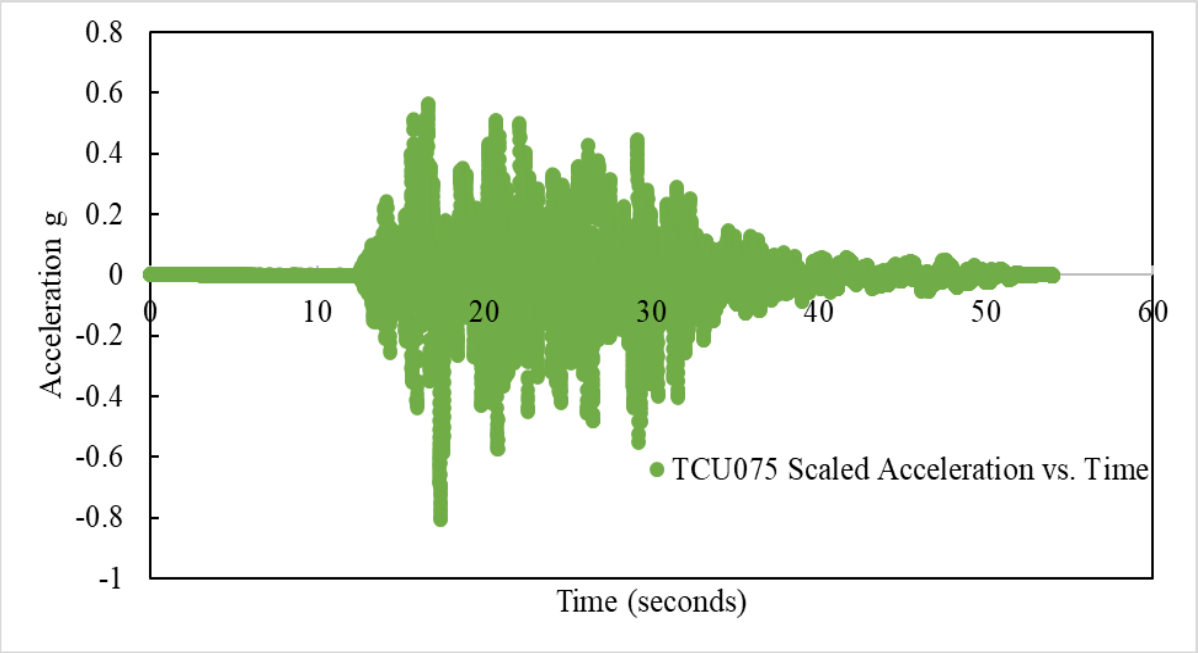

(a)

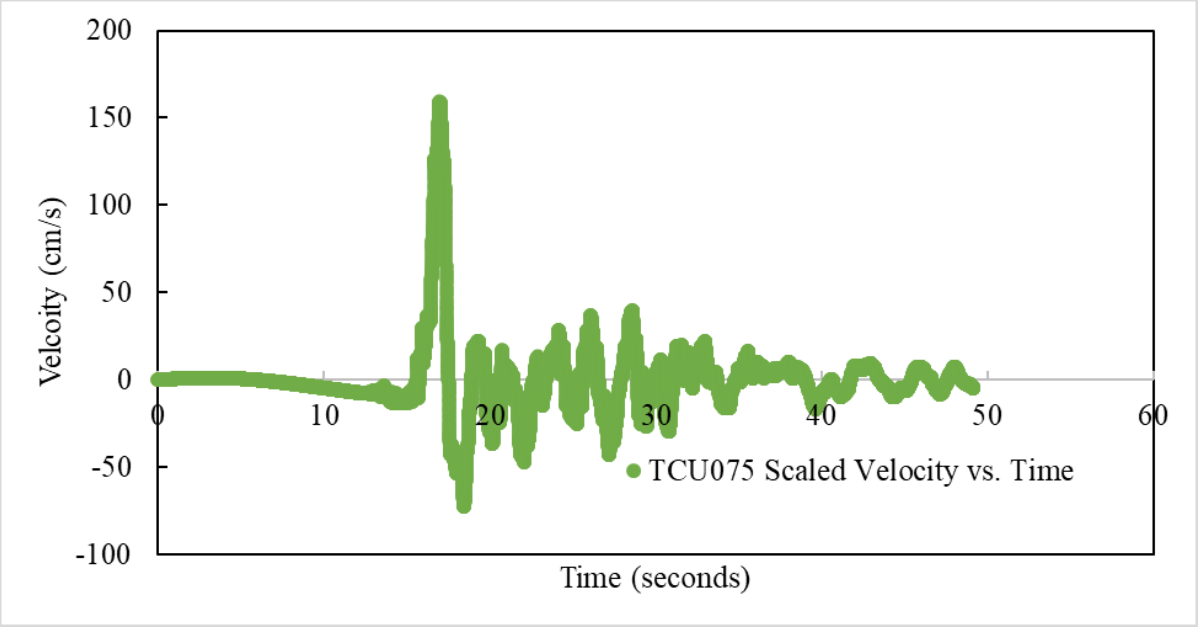

(b)

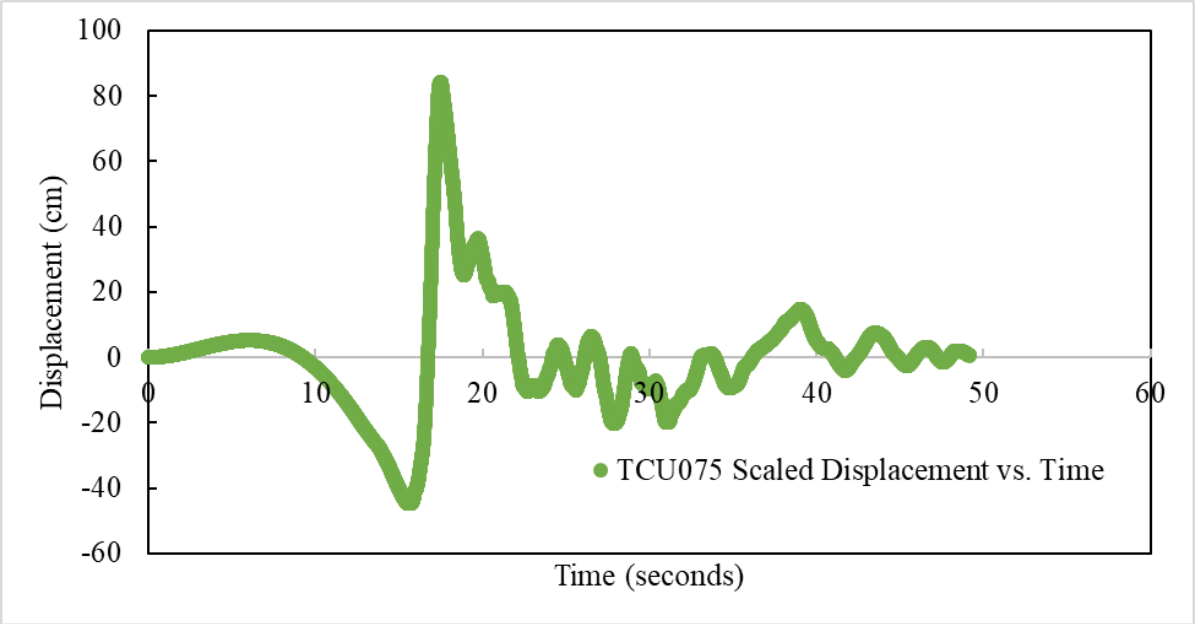

(c)

The fatigue properties applied were E_0 = 0.159 and m = -0.453 for a slenderness ratio (L/D) of 7. The numerical simulation results were compared with experimental data by Chang et al. to validate the proposed numerical models and to calculate the corresponding damage indices. Comparisons of hysteresis curves between nonlinear time-history analysis results and experimental tests of Specimen B from Chang et al. are shown in Figures 7a–7d. Experimental results detected some flexural cracks and some concrete cover spalling. Overall, Specimen B was not severely damaged. The proposed numerical models were compared with experimental testing results. All four numerical models are optimal to assess the seismic performance of RC single-column pier-supported bridges. The proposed damage indices can reflect the damage states in accordance with the experimental results.

Models 1 (without bond-slip and without fatigue) and 2 (without bond-slip and with fatigue) demonstrated hysteresis curves that aligned well with the experimental results, but they have slightly higher predicted stiffness, as shown in Figures 7a and 7b.

Model 3 (with bond-slip and without fatigue) developed a symmetrical hysteresis curve, as shown in Figure 7c. In addition, Model 3 had a stronger pinching effect due to bond-slip in comparison to Model 1 (without bond-slip and without fatigue).

In Figure 7d, the overall hysteresis curve of Model 4 (with bond-slip and with fatigue) aligned well with experimental data for Specimen B, especially in the predictions of strength and stiffness. The predicted hysteresis curve demonstrated a slight pinching effect due to bond-slip and could capture strength/stiffness degradation due to the low-cycle fatigue of longitudinal steel rebars. However, it is noted that the simulation results of Model 4 showed strong strength/strength degradations closer to the end of the ground motion time duration.

Figure 7. Comparison of Hysteresis Curves between Nonlinear RHA Results and Pseudo-dynamic Tests of Specimen B by Chang et al. [19] for (a) Model 1, (b) Model 2, (c) Model 3, and (d) Model 4

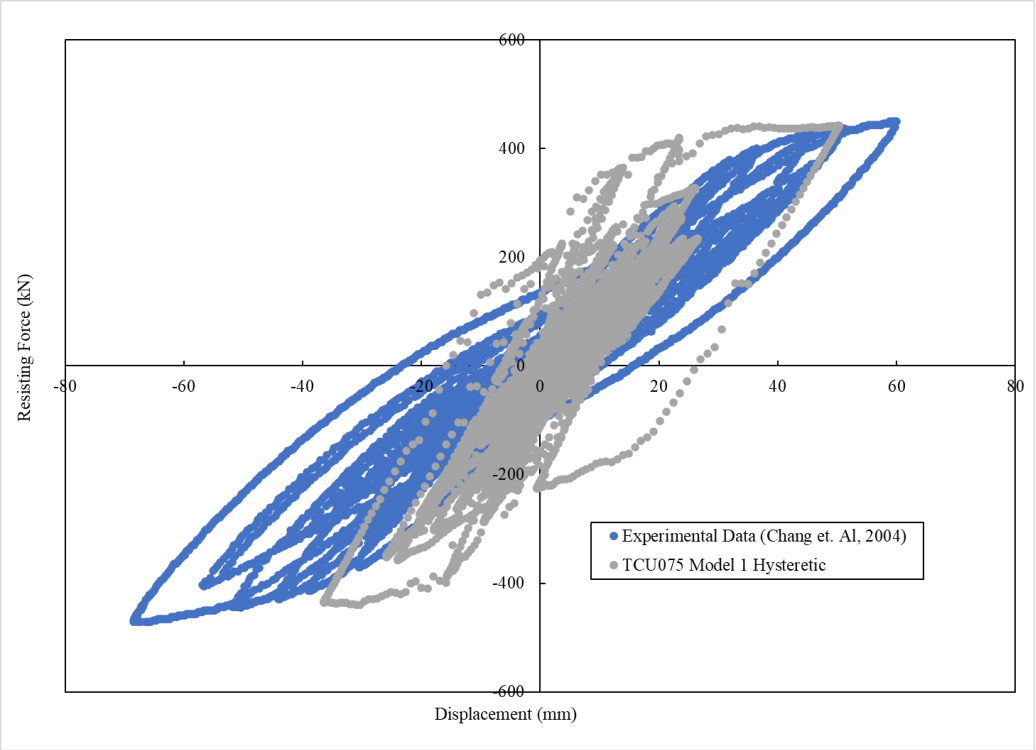

(a)

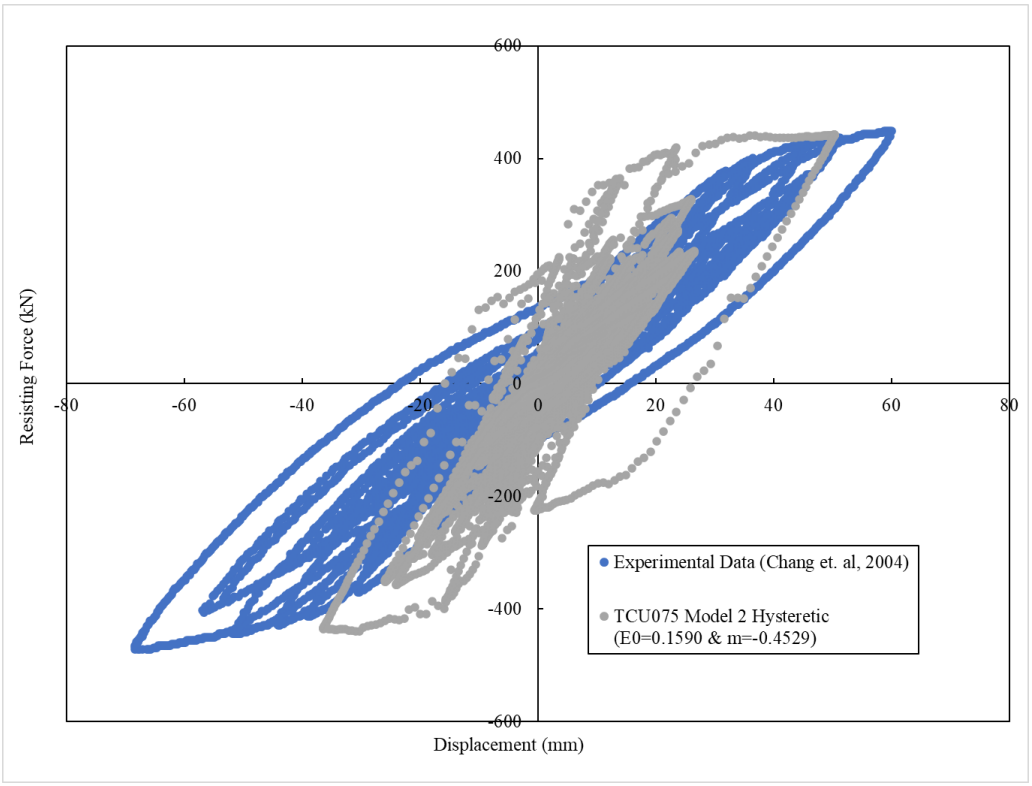
600
400
200
0
-200
-400
-600
-80
-60
-40
-20
0
20
40
60
80
Resisting Force (kN)
Displacement (mm)
Experimental Data (Chang et. al, 2004)
TCU075 Model 2 Hysteretic
(E0=0.1590 & m=-0.4529)

(b)

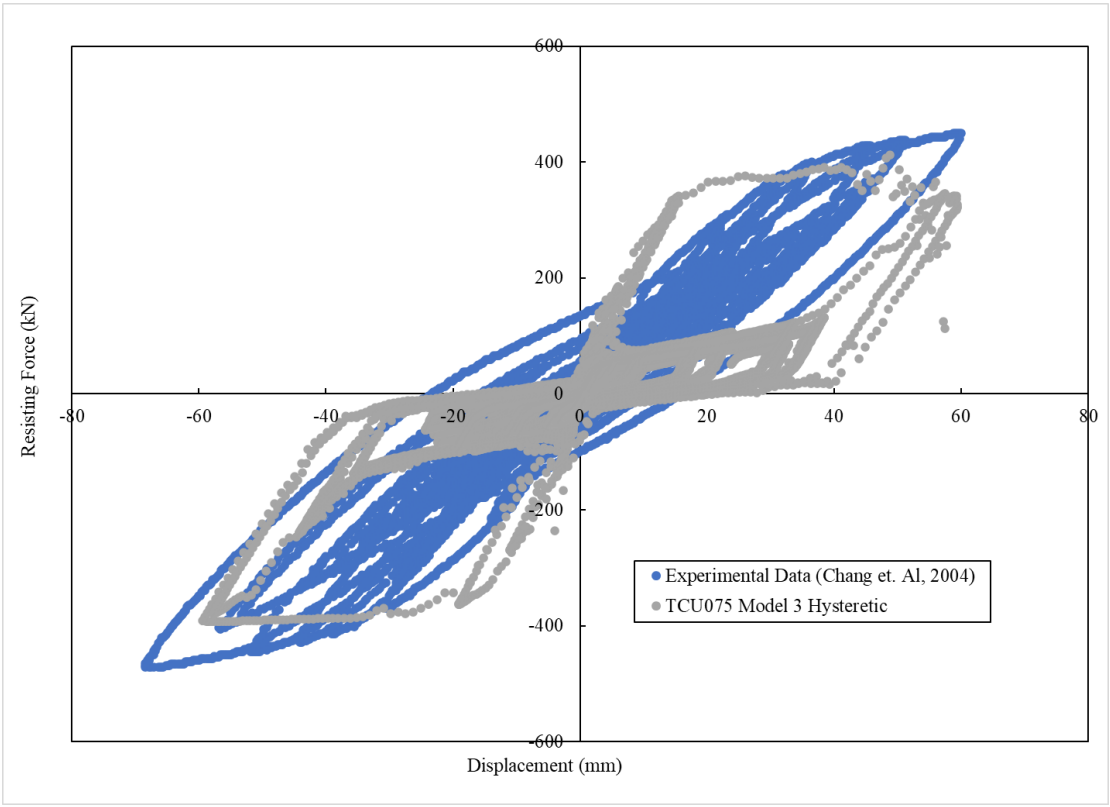
600
400
200
0
-200
-400
-600
-80
-60
-40
-20
0
20
40
60
80
Resisting Force (kN)
Displacement (mm)
Experimental Data (Chang et. Al, 2004)
TCU075 Model 3 Hysteretic

(c)

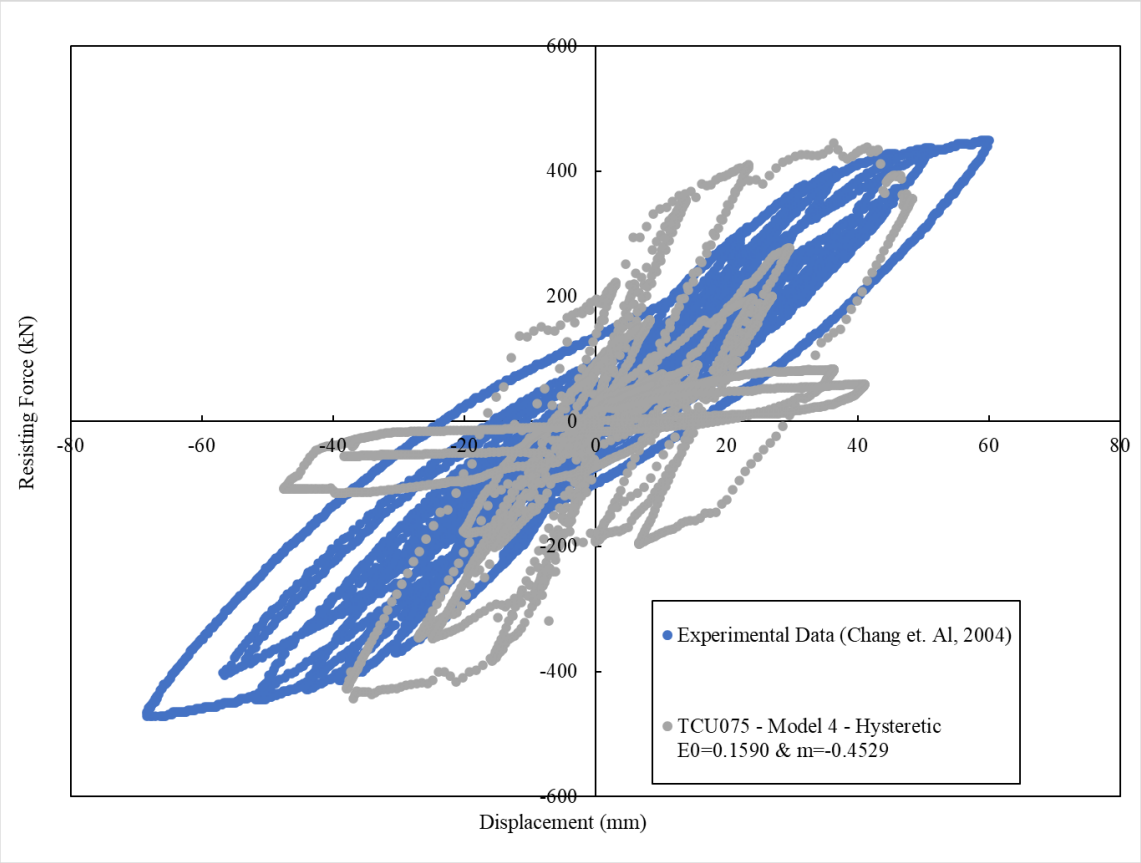
600
400
200
0
-200
-400
-600
-80
-60
-40
-20
0
20
40
60
80
Resisting Force (kN)
Displacement (mm)
Experimental Data (Chang et. Al, 2004)
TCU075 - Model 4 - Hysteretic
E0=0.1590 & m=-0.4529

(d)

6. Numerical Simulations of Damage Indices and Performance Assessments

The numerical simulations of damage indices corresponding to Figures 7a, 7b, 7c, and 7d are illustrated in Figures 8, 9, 10, and 11, respectively.

Figure 8 shows the cover concrete damage index D_c. Models 1 and 2 show similar results in which the 2 curves almost overlap. Models 3 and 4 show different results. Notably, Model 3 shows small D_c values. Model 4 shows similar results to Models 1 and 2 up to around t = 44 sec. Model 4 shows D_c = 1.0 at around t = 48 sec., which is closer to the end of the ground motion time duration.

The steel strain damage index D_{ss} is shown in Figure 9. Models 1 and 2 show similar results in which the 2 curves almost overlap. Models 3 and 4 show different results. Model 4 shows similar results to Models 1, 2, and 3 up to around t = 39 sec. Model 4 shows D_{ss} = 1.0 at around t = 39 sec. It is noted that D_{ss} of Models 1 and 2 have larger values than those of Models 3 and 4 mainly due to bond-slip effect.

Figure 10 demonstrates the steel low-cycle fatigue damage index D_{sf}. D_{sf} of Model 2 shows a larger value than that of Model 4. It is noted that Model 4 shows D_{sf} = 1.0 at around t = 39 sec.

The section damage index $D_{section}$ is shown in Figure 11. Models 1 and 2 show similar results in which the two curves almost overlap. Model 4 shows similar results to Models 1, 2, and 3 up to around t = 39 sec. Model 4 shows $D_{section}$ = 1.0 at around t = 39 sec. It is noted that the section damage index $D_{section}$ of Models 1, 2, and 3 is governed by D_{ss}. The section damage index $D_{section}$ of Model 4 is governed by D_c.

The simulated section damage index $D_{section}$ of all four numerical models is between 0.1 and 0.2 for Specimen B. According to Table 2, the bridge column is classified as “minor damage” and could remain operational. All four numerical models align well with the experimental test results.

The effects of bond-slip, cover concrete damage, steel strain damage, global buckling, and low-cycle fatigue damage of steel rebars would impact and influence the seismic behavior of RC bridge columns.

Figure 8. Cover Concrete Damage Index (D_c) of Models 1, 2, 3, and 4

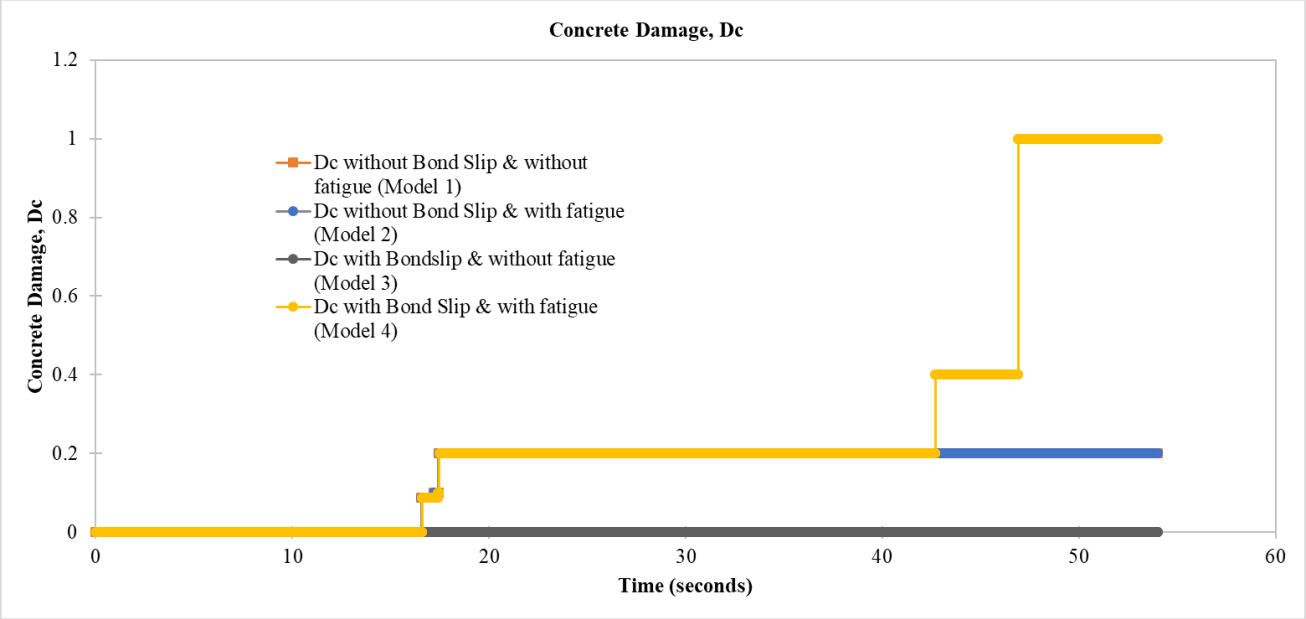

Figure 9. Steel Strain Damage Index (D_{ss}) of Models 1, 2, 3, and 4

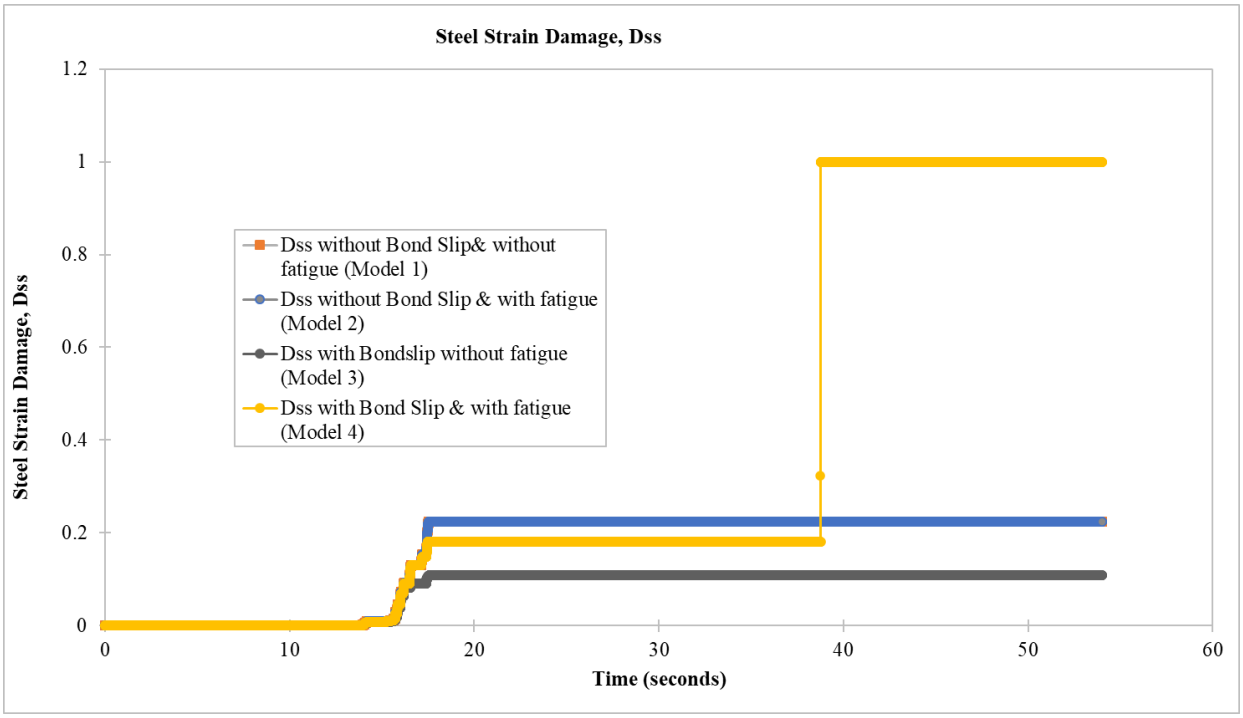

Figure 10. Steel Low-Cycle Fatigue Damage Index (D_{sf}) of Models 2 and 4

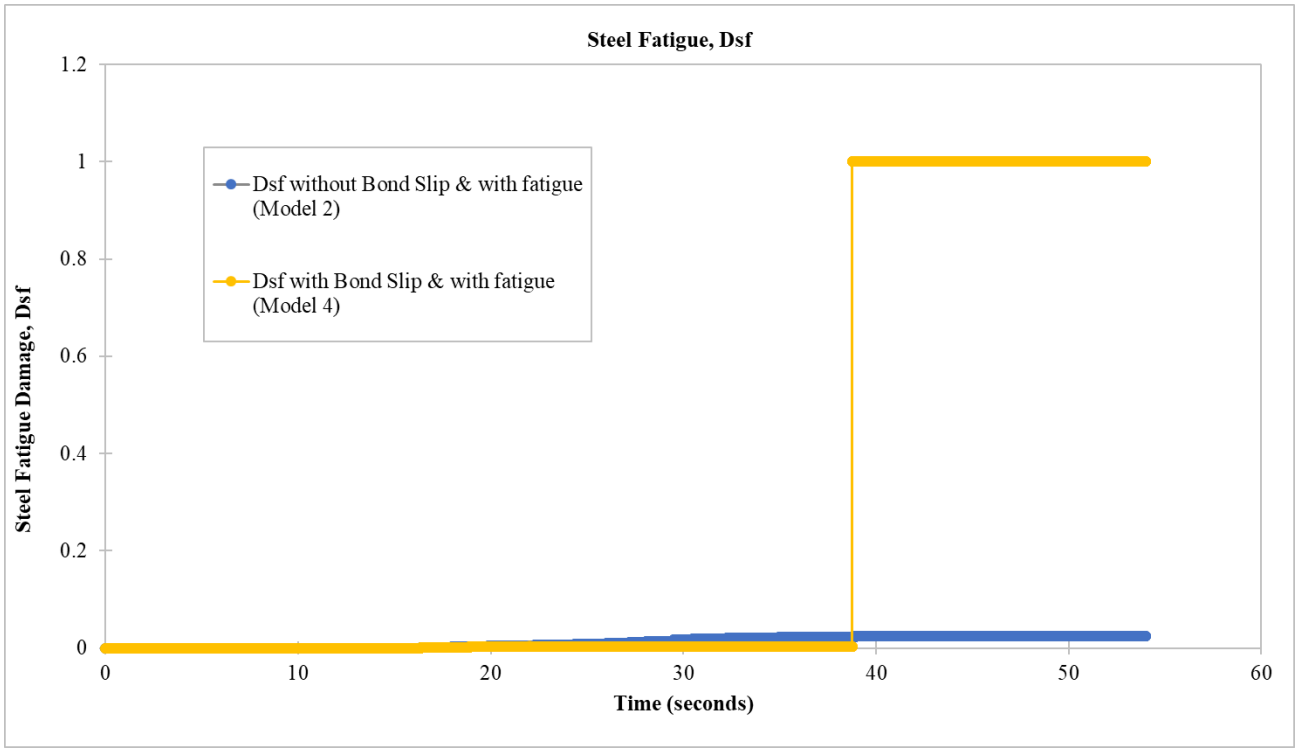

Figure 11. Section Damage Index ($D_{section}$) of Models 1, 2, 3, and 4

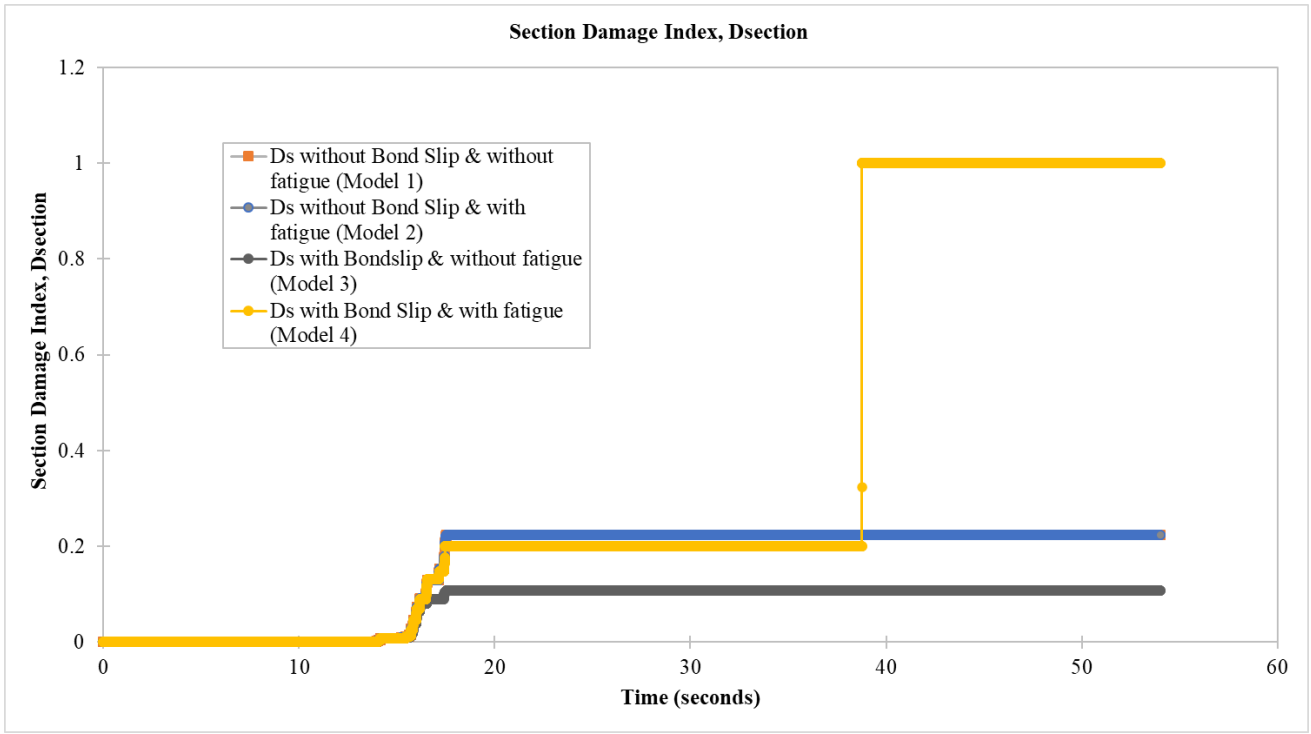

7. Summary & Conclusions

This study investigated the effects of low-cycle fatigue fracture of longitudinal reinforcing steel bars on the seismic performance of reinforced concrete bridge piers. Detailed understandings of low-cycle fatigue failure of steel reinforcement of RC bridge piers subjected to seismic loadings were achieved by also incorporating the effect of inelastic buckling in terms of slenderness ratio.

Damage indices were utilized to assess the seismic performance of RC single-column pier-supported bridges with flexural failure under near-fault ground motion. The damage indices can numerically assess the damaged state of RC bridge piers and show the gradual accumulation of damage. Four numerical models were developed with fiber-based, nonlinear beam-column elements to conduct the seismic assessments.

The four numerical models were developed with different considerations of low-cycle fatigue and bond-slip: Models 1 (without bond-slip and without fatigue), 2 (without bond-slip and with fatigue), 3 (with bond-slip and without fatigue), and 4 (with bond-slip and with fatigue). The models considered various damage parameters such as the low-cycle fatigue, tensile strain damage, global buckling of longitudinal steel bars, the cracking and spalling of cover concrete, and the bond-slip between concrete and longitudinal steel bars.

According to the simulation results of this study, the simulated section damage index $D_{section}$ of all four numerical models align well with both experimental test results and the National Cooperative Highway Research Program Synthesis 440 [36] for bridge performance assessment. Furthermore, the predicted seismic responses of all four numerical models are in good agreement with experimental test results. The proposed damage indices can reflect the damage states in accordance with the experimental results. Thus, all four numerical models are optimal to assess the seismic performance of RC single-column pier-supported bridges.

It is shown that the proposed numerical models effectively capture the damage states and failure of RC single-column pier-supported bridges when compared with experimental testing results. Moreover, the damage values reflect the damage development states in accordance with the experimental test results. Based on the simulation results of this study, bond-slip, cover concrete damage, steel strain damage, global buckling, and low-cycle fatigue damage of steel rebars demonstrated strong impact and influence on the seismic behavior of RC bridge columns.

The proposed numerical models have demonstrated to be capable of capturing the damaged evolution of RC bridge piers under seismic events, can help predict the damage states and seismic behavior of RC bridge columns, and could be a boon to those performing non-linear analysis and performance assessment of RC bridge structures.

Far too many bridges and the transportation system have been damaged by earthquakes. This study is expected to advance the state of bridge and highway engineering and will provide improved tools

to assess the vulnerability of bridges and highway systems in a cost-effective, timely, and efficient way. This study will mitigate risk and improve earthquake resilience for RC bridges. Therefore, this study will not only benefit the engineering community, but also the publicwith enhanced safety, economy, and transportation security.

The proposed numerical models with low-cycle fatigue fracture could also provide future applications for non-linear analysis of other types of RC bridges and RC building structures for the purpose of damage assessment.

Bibliography

1. Mergos, P. E., and Kappos, A. J. (2013). A combined local damage index for seismic assessment of existing RC structures. *Earthquake Engineering and Structural Dynamics* 42(6): 833-852.

2. Park, Y., and Ang, A. H. (1985). Mechanistic seismic damage model for reinforced concrete. *J Struct Eng* 111(4): 722–39.

3. Park, Y., Ang, A. H., and Wen, Y. (1987). Damage-limiting aseismic design of buildings. *Earthq Spectra* 3(1): 1–26.

4. Heo, Y., and Kunnath, S. K. (2013). Damage-based seismic performance evaluation of reinforced concrete frames. *Int J Concr Struct Mater* 7(3): 175–82.

5. Williams, M. S., and Sexsmith, R. G. (1995). Seismic damage indices for concrete structures: a stateof- the-art review. *Earthq Spectra* 11(2): 319–49.

6. Su, J.S., Dhakal, R. P., and Wang, J. (2017). Fiber-based damage analysis of reinforced concrete bridge piers. *Soil Dynamics and Earthquake Engineering*:96,13–34.

7. Babazadeh, A., Burgueño, R., and Silva, P. F. (2015). Use of 3d finite-element models for predicting intermediate damage limit states in rc bridge columns. *J Struct Eng* 141(10).

8. Kashani, M. M., Lowes, L.N., Crewe, A. J., and Alexander, N. A. (2016). Nonlinear fiber element modelling of rc bridge piers considering inelastic buckling of reinforcement. *Eng Struct* 116: 163–77.

9. Tripathi, M., Dhakal, R. P., Dashti, F, and Massone, L.M. (2019). "Low-cycle Fatigue Damage of Buckling Prone Reinforcing Bars." *New Zealand Society for Earthquake Engineering*, 1–9.

10. Stone, W. C., and Taylor, A. W. (1993). *Seismic performance of circular bridge columns designed in accordance with aashto/caltrans standards*. NISIT building Science Series 170, National Institute of Standards and Technology, Gaithersburg, MD.

11. Stone, W. C., and Taylor, A. W. *Performance evaluation database for concrete bridge components and systems under simulated seismic loads*. PEER Report 1999/11, Pacific Earthquake Engineering Research Center, Berkeley, CA; 1999.

12. Goodnight, K., M. J., and Nau, J. M. (2016). Strain limit states for circular RC bridge columns. *Earthquake Spectra* 32(3): 1627–1652.

13. McKenna, F., Fenves, G. L., and Scott, M. H. (2000). *Open system for earthquake engineering simulation*. University of California, Berkeley, CA.

14. Sharifi, A., Banan, M., and Banan, M. (2012). A strain-consistent approach for determination of bounds of ductility damage index for different performance levels for seismic design of rc frame members. *Eng Struct* 37: 143–51.

15. Yue, J., Qian, J., and Beskos, D. E. (2016). A generalized multi-level seismic damage model for rc framed structures. *Soil Dyn Earthq Eng* 80: 25–39.

16. Ding, Y., Wu, D., Su, J., Li, Z.-X., Zong, L., & Feng, K. (2021). Experimental and numerical investigations on seismic performance of RC bridge piers considering buckling and low-cycle fatigue of high-strength steel bars. *Engineering Structures*, *227*, 111464.

17. Kashani, M. M., Barmi, A. K., & Malinova, V. S. (2015). Influence of inelastic buckling on low-cycle fatigue degradation of reinforcing bars. Construction & Building Materials, 94, 644–655.

18. Su, J., Wu, D., & Wang, X. (2023). Influence of ground motion duration on seismic behavior of RC bridge piers: The role of low-cycle fatigue damage of reinforcing bars. Engineering Structures, 279, 115587.

19. Chang, Y. S., Li, Y. F., and Loh, C. H. (2004). Experimental study of seismic behaviors of as-built and carbon fiber reinforced plastics repaired reinforced concrete bridge columns. *J Bridge Eng ASCE* 9(4): 391–402.

20. Loh, C. H., Wan, S., and Liao, W. I. (2002). Effects of hysteretic model on seismic demands: consideration of near-fault ground motions. *Struct Des Tall Build* 11: 155–169.

21. Ansari, M., Daneshjoo, F., and Mohammadi, M. S. (2017). On estimation of seismic residual displacements in reinforced concrete single column bridges through force-displacement method. *Int J Civil Eng* 15: 473–486.

22. Yi, W. J., Zhou, Y., Hwang, H. J., Cheng, Z. J., and Hu, X. (2018). Cyclic loading test for circular reinforced concrete columns subjected to near-fault ground motion. *Soil Dyn Earthq Eng* 112: 8–17.

23. Cao, V.V. (2019). Characterization of near-fault effects on potential cumulative damage of reinforced concrete bridge piers. *Int J Civil Eng* 17: 1603–1618.

24. Xia, C., and Liu, C. (2020). Influence of the multi-pulse near-fault earthquake motion on the seismic risk evaluation for reinforced concrete bridge. *Nat Hazards* 102: 759–782.

25. Pang, Y. T., Cai, L., and Zhong, J. (2020). Seismic performance evaluation of fiber-reinforced concrete bridges under near-fault and far-field ground motions. *Structures* 28: 1366–1383.

26. Seyed Ardakani, S. M., Saiid Saiidi, M., and Somerville, P. (2021). Residual drift spectra for RC bridge columns subjected to near fault earthquakes. *Earthq Eng Eng Vib* 20: 193–211.

27. Phan, V., Saiidi, M. S., Anderson, J., & Ghasemi, H. (2007). Near-Fault Ground Motion Effects on Reinforced Concrete Bridge Columns. *Journal of Structural Engineering (New York, N.Y.)*, *133*(7), 982–989.

28. Todorov, B. and Billah, A. H. M. M. (2021). Seismic fragility and damage assessment of reinforced concrete bridge pier under long-duration, near-fault, and far-field ground motions. *Structures (Oxford)*, *31*, 671–685.

29. Park, R., and Paulay, T. (1975). *Reinforced concrete structures*. Wiley, New York.

30. Girard, C., and Bastien, J. (2002). Finite-element bond-slip model for concrete columns under cyclic loads. *J Struct Eng ASCE* 128(12): 1502–1510.

31. Zhao, J., and Sritharan, S. (2007). Modeling of strain penetration effects in fiber-based analysis of reinforced concrete structures. *ACI Struct J* 104(2): 133–141.

32. Gomes, A., and Appleton, J. (1997). Nonlinear cyclic stress-strain relationship of reinforcing bars including buckling. *Eng Struct* 19(10): 822–826.

33. Dhakal, R. P., and Maekawa, K. (2002). Modeling for postyield buckling of reinforcement. *J Struct Eng ASCE* 128(9): 1139–1147.

34. Paulay, T., and Priestley, M. J. N. (1992). *Seismic design of reinforced concrete and masonry buildings*. Wiley, New York.

35. Priestley, M. J. N., Seible, F., and Calvi, G.M. (1996*). Seismic design and retrofit of bridges*. Wiley-Interscience, New York.

36. Transportation Research Board. (2013). Performance-based seismic bridge design, Rep. No. Synthesis 440. National Cooperative Highway Research Program, Washington, DC.

37. Hisham M. and Yassin M. (1994). *Nonlinear Analysis of Prestressed Concrete Structures under Monotonic and Cycling Loads*. PhD dissertation, University of California, Berkeley, 1994.

38. Chang, G., and Mander, J. (1994). *Seismic energy based fatigue damage analysis of bridge columns: part I—evaluation of seismic capacity*. NCEER Technical Report 94-0006.

About the Authors

Yu-Fu Ko, PhD, PE

Dr. Ko joined the California State University, Long Beach (CSULB) Civil Engineering and Construction Engineering Management Department in Fall 2009. He received his B.S. degree in Structural Engineering from National Taiwan University of Science and Technology and his MS and PhD degrees (as an outstanding PhD award recipient) in Civil Engineering, focusing on Structural Mechanics and Structural Engineering/Dynamics from the University of California, Los Angeles (UCLA). Prior to joining CSULB, Dr. Ko was a postdoctoral researcher and lecturer at UCLA and a senior structural design engineer at Englekirk and Sabol Consulting Structural Engineers, Inc. He is a registered Professional Civil Engineer in the state of California. Dr. Ko's areas of research include micro/nano-mechanics modeling of heterogeneous composite materials, micromechanical damage mechanics modeling and associated applications, damage assessment and experimental mechanics of structural materials, nonlinear/linear structural dynamic analysis of structures subjected to earthquake motions, finite element method code-based and performance-based structural design of structures, and seismic retrofitting of existing structures. He has presented at national and international conferences and published research papers in national and international peer-reviewed journals. He actively participates in ASCE, ASME, AISC, ACI, SEAOSC, IACM, USACM, and other national and international societies. He is also a peer reviewer for numerous technical journals.

Jessica Gonzalez, EIT

Jessica Gonzalez is a research graduate assistant working with Dr. Yu-Fu Ko at California State University, Long Beach (CSULB). She received her B.S. in civil engineering from CSULB with cum laude degree honors and is currently enrolled as a graduate student working towards her master's degree. She is certified as an Engineer-in-Training (EIT) and is currently employed as a structural designer at RailPros, Inc. Her research interests are finite element modeling of bridges and the seismic analysis of bridge components. Additionally, her software skills include AutoCAD and OpenSees.

MTI FOUNDER

Hon. Norman Y. Mineta

MTI BOARD OF TRUSTEES

Directors